

A Novel 3D Reconstruction Approach from Uncalibrated Multiple Views Based on Homography

Shuai Liu, Lingli Zhao, Junsheng Li

School of Engineering, Honghe University, Mengzi, China, 661100 Email: liushuai_csu@126.com

Li Ma

Changjiang Institute of Survey, Planning, Design and Research, Wuhan, Hubei, China, 430010

Abstract—In this paper, we focus on a kind of 3D object shape reconstruction from images and put forward a metric approach to recover the object based on slicing planes by homography transformation and image consistency between multiple images. This approach done here eliminates the requirement for camera calibration, the estimation of the fundamental matrix, feature matches and pose estimation. We adopt a set of hypothetical planes to intersect the reconstructed object to obtain every slicing plane of the reconstructed object by homography transformation and recover it to 3D adding vanishing points by the constraints of silhouette and the scene. The experiment shows that the approach is much validated, and something useful is obtained.

Index Terms—Homography, 3D Recovery, 2D images, slicing planes

I. INTRODUCTION

Three-dimensional (3D) object reconstruction from multiple images has been an important hotspot in the field of computer vision and close-range photogrammetry. Measurement of geometrical entities by vision technique has attracted a lot of attention in the world recently and received wide applications in recent years[1,2,3], including architectural and indoor measurement, reconstruction from paintings, forensic measurement, traffic accident investigation, industrial applications, cultural heritage, widely available image collections on the Internet and publicly available applications such as Google Earth and Microsoft Photosynth etc.

The conventional 3D measurable reconstruction requires the cameras calibration and pose based on matching points, and then is reconstructed by triangulation of back-projected image points in the object space. If the Euclidean reconstruction of a scene is obtained, then any geometrical information about the scene can be measured accordingly. However, this kind of methods, explicitly require camera pose and calibration, and enough number of point correspondences between the images. The errors introduced by matching and camera calibration may propagate along the

computational chain and cause a loss of accuracy to the final results.

Visual hull based methods attempt to fuse silhouette information from multiple views in 3D space thereby requiring calibrated views [4] [5] [6]. However, camera calibration itself is a challenging problem with a large literature devoted to it. There are many situations in real life where calibration is the most cumbersome task that should be avoided. A common case is multiple non-stationary cameras (with possibly different internal parameters) in the absence of calibration pattern are used to capture different views of an object.

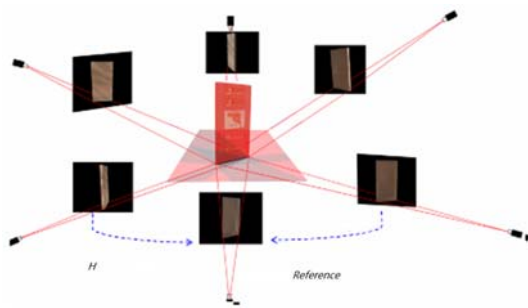
In the recent years, the implied 3D scene information can be retrieved from 2D images by the homography transformation and can be utilized for use in many applications, including tracking people [7], shadow removal, and detecting low-lying objects [8]. Although some techniques have conceptually been proven to be successful in certain cases [9] [10] [11], their use is limited due to specific requirements. Various papers which are dedicated to the problem of 3D object shape recovery have utilized the properties of the homography transformation and the silhouette images to solve the aforementioned problems [12] [13]. The homography transformation provides a strong geometric constraint and is comparatively simple.

The approach done here based on the constraints of silhouette and the scene, a group of hypothetical planes are set to intersect the reconstructed object to obtain slicing planes of the reconstructed object by homography transformation and are used to recover 3D model, moreover calculate the reconstructed object height by reference height. This approach requires no camera calibration, the estimation of the fundamental matrix or feature matches; hence, it reduces the computational complexity. The experiment shows that the approach is much validated, and something useful is obtained.

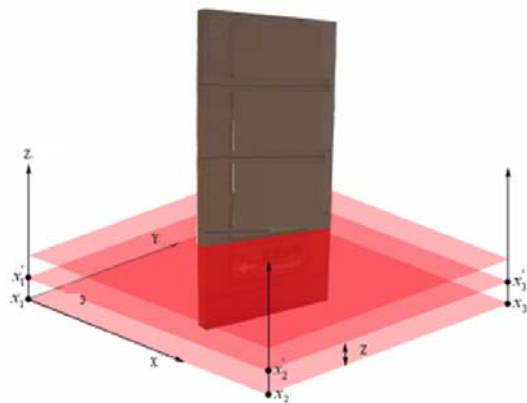
II. THREE-DIMENSIONAL RECONSTRUCTION BASED ON SLICING PLANES

The slicing planes reconstruction algorithm shows in Figure 1, which needs SETOI operation, shown in Figure

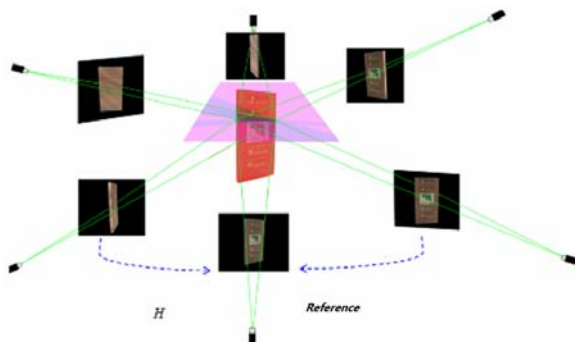
2. Multiple images are captured around the reconstructed object. The reconstructed object imaging contours are obtained by image segmentation (*Segment*). That is the course of SETOI, *Selecting* an image as a reference image (shown in Figure 1 (a)), *extracting* (Feature extraction) four points as control points, *binarizing* the images of reconstructed object and *transforming* other images onto the reference image by homography values, finally *overlaying* and *intersecting*. Increase two control points (etc. x_1, x_3 shown in Figure 1 (b)) along the Z-axis direction in the original plane of four control points (x_1, x_2, x_3, x_4 shown in Figure 1 (b)), then four control points in any new layer are calculated. Those points of every layer can formed a new parallel plane to obtain new slice. Those slices of different images can stack together to constitute the contour of object reconstructed through SETOI operation, shown in Figure 1(d).



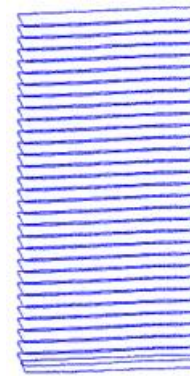
(a)The result of SETOI for the first layer



(b) A set of hypothetical planes to intersect the reconstructed object



(c) One of the SETOI results of SETOI



(d) The shape from SETOI

Figure 1. The schematic diagram of slicing planes reconstruction approach

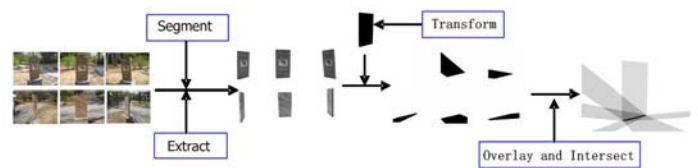


Figure 2. The schematic diagram of obtaining slicing planes by SETOI

The reconstruction algorithm based on slicing planes follows the classical collinear equation, and the Vanishing Point Theory.

A camera is a mapping between the 3D world (object space) and a 2D image. A point in space is represented in the homogeneous coordinates by $X = (X, Y, Z, 1)$, which is mapped to the point x on the image plane which is a line joining of the point X and the center of projection to the image plane.

By the projection relations, we could get the relations are:

$$\lambda x_i = P X_w = [p_1 \quad p_2 \quad p_3 \quad p_4] \begin{bmatrix} X \\ Y \\ Z \\ 1 \end{bmatrix} \quad (1)$$

When the point in the object space lies on the ground plane such that $Z = 0$, the linear mapping given in formula (1) will reduce to the planar homography:

$$s x_i = H_i X_w = [p_1 \quad p_2 \quad p_4] \begin{bmatrix} X \\ Y \\ 1 \end{bmatrix} \quad (2)$$

Where H_i is the homography matrix, which is a direct mapping of the points lying on a plane in the object space across different images. This formulation introduces another scaling factor s to the mapping equation which stems from $Z = 0$. While equation (2) is defined for $Z = 0$, the same relation can be derived for any other plane in the object space:

$$x_i = H_{wi} X_w = H_{wi} (H_{wj}^{-1} X_j) = H_{ij} x_j \quad (3)$$

Where H_{ij} is the homography matrix describing the projective transformation of the pixels lying on image planes i and planes j . The estimation of this

transformation up to a scale factor requires a minimum of four points lying on the plane. We should state that it is these discrepancies, or the so called shadow projections, that will let us estimate the 3D shape of the object. Homography should have a strong binding geometry.

H_{Π} is the homography between two images taken from different angles shown in Figure 3. Pixels in image 1 can be transformed onto image 2 by H_{Π} .

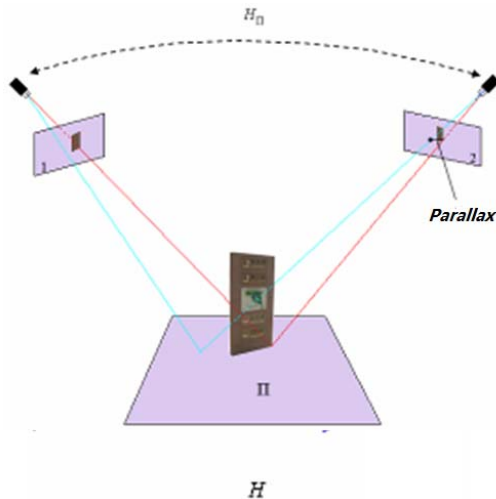


Figure 3. The schematic diagram of homograph geographic constraint

By equation (1) it can be obtained:

$$\lambda_i x'_i = [p_1 \quad p_2 \quad p_4] \begin{bmatrix} X_i \\ Y_i \\ 1 \end{bmatrix} + p_3 Z \quad (4)$$

The vanishing point of p_3 corresponds to the vanishing point in the direction of the Z axis, combining with equations (2) it provides:

$$\lambda_i x'_i = s_i x_i + v_z Z \quad (5)$$

The unknowns of the above equation are λ_i and s_i ,

$$\begin{bmatrix} \lambda_i \\ s_i \end{bmatrix} = (A_i^T A_i)^{-1} A_i^T b_i \quad (6)$$

Where $A_i = [x'_i \mid -x_i]$, $b_i = v_z Z$, once s_i is calculated, coordinates of the image points along the straight line $x_i v_z$ can be deduced. Then the control points of new layer can be calculated shown in Figure 4, and the homography vector between new layers can be calculate.

There are two reasons mainly adopting vanishing point: First, straight lines parallel to the ground after imaging intersect at two vanishing points v_1 and v_2 , vanishing line is l_v , parallel lines perpendicular to the ground intersect at the vanishing point v_z seen in Figure 5, it can be substituted into equation (4). Second, vanishing

points can be used to deduce the image invisible control points of a new layer. For example, the points x_4, x'_2, x'_4 are blocked, seen in Figure 1(b). The vanishing point can be calculated by the parallel straight-line imaging.

$$\begin{cases} v_1 = (x_1 \times x_4) \times (x_2 \times x_3) \\ v_2 = (x_1 \times x_2) \times (x_3 \times x_4) \\ v_z = (x_1 \times x'_1) \times (x_3 \times x'_3) \end{cases} \quad (7)$$

Where x_4 is cannot be seen, but the vanishing point v_1 and v_2 can be calculated by the lines l_{14} and l_{34} . So equation (7) provides the following relation:

$$\begin{cases} x_4 = (x_1 \times v_1) \times (x_3 \times v_2) \\ x'_2 = (x_2 \times v_z) \times (x'_3 \times v_1) \\ x'_4 = (x_2 \times v_z) \times (x'_3 \times v_1) \end{cases} \quad (8)$$

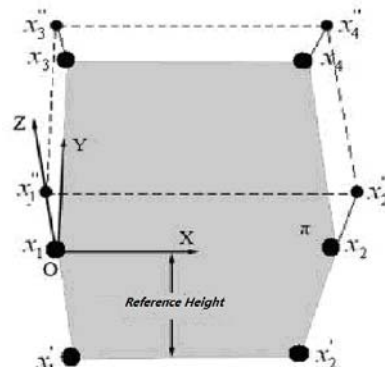


Figure 4. The schematic diagram of hierarchy control points

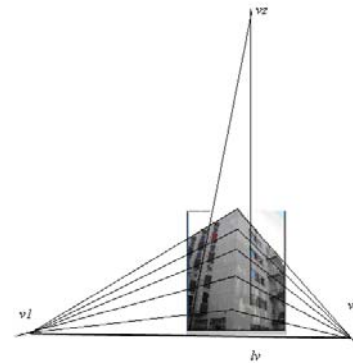


Figure 5. Parallel lines in the reality projected to the image intersect one point

III. THREE-DIMENSIONAL RECONSTRUCTION ALGORITHM BASED ON SLICES

A. Space Layer Control Point Deduction and Slices Generation

Algorithm 1: the layer control points calculation

Condition: Given image coordinates x_i ($i=1,2,3,4$) of four control points on the plane ($Z=0$), and two points image coordinates x'_i and x'_j on the plane ($Z=Z_0$).

Objective: Calculate image coordinates of the four control points on the layer $Z = Z_1$ ($Z_1 \neq 0, Z_1 \neq Z_0$). Steps:

- a) Calculate the vanishing point in three directions: v_x, v_y and v_z ;
- b) Calculate the scaling factors of the two lines ($X_i X_i'$) towards the Z-axis direction;
 v_z, x_i and x_i' are substituted into equation (5) to obtain two scaling factors.
- c) Calculate image plane coordinates of two points in the two Z-axis direction lines (straight line $X_1' X_1, X_2' X_2$ as shown in Figure 4) on the plane ($Z=Z_1$). Substitute the scaling factors calculated by the step b) are into equation (5) to obtain: $\lambda_i'' x_i'' = s_i x_i + v_z Z_1$, then turn the equation of the right side into homogeneous coordinates, we can obtain x_i'' .
- d) Calculate image plane coordinates of another two points on the layer of the plane ($Z=Z_1$) by Vanishing Point formula.

Algorithm 2: horizontal slice generation

Conditions: Given the grayscale contours images of reconstructed object, and the four control points on the layer ($Z=Z_1$) and the two points in the perpendicular direction of each image.

Objective: Calculate the overlay results of all the contours images projected onto the reference image on the layers of the plane ($Z=Z_i, i = 1, 2, 3 \dots n$). Steps:

- a) In each image, Algorithm 1 is adopted to calculate 4 image control points in the layer ($Z=Z_i$);
- b) First, select reference image, then according to four image points of in the layers ($Z=Z_i$) in each image obtained in step a, and calculate the homographies between reference image and other images;
 $x_{ref}^k = H_{ref}^j x_j^k$, where $k=1,2,3,4$, H_{ref}^j is the homography between image j and the reference image.
- c) Obtain the slice of layer I by SETOI operating from these gray-scale images.

B. The Reconstruction of the Three-dimensional Horizontal slice and the Height Calculation of Reconstructed Object

$p_3 = v_z$ is put into the equation (4) to provide the following relation:

$$\lambda_i x_i' - v_z Z_1 = \begin{bmatrix} p_1 & p_2 & p_4 \end{bmatrix} \begin{bmatrix} X_i \\ Y_i \\ 1 \end{bmatrix} = H_{z1} \begin{bmatrix} X_i \\ Y_i \\ 1 \end{bmatrix} \quad (9)$$

λ_i is a scaling factor, which is calculated by algorithm 1, so does x_i', Z_1 can be set to a constant, the premise is that the value does not exceed the height of the reconstructed object Z-axis coordinate value of the reference image.

Algorithm 3: the three-dimensional restoring coordinates of the horizontal slice

Conditions: Given the grayscale images of overlaying and intersecting in the layer ($Z=Z_1$), and the four control points and four scaling factors $\lambda_1, \lambda_2, \lambda_3, \lambda_4$.

Objective: Recover three-dimensional coordinates of the hierarchical contour points in the layer ($Z=Z_1$).

- a) Calculate homography between the layer ($Z=Z_1$) and the other images; The four control points and the scaling factor are substituted into equation (9) to obtain homography H_{z1} .
- b) Extract overlaying grayscale images;
- c) Restore the three-dimensional coordinates (X_i, Y_i, Z_i) of the contour points of the layer ($Z=Z_1$). The image coordinates of the extracted contour points are substituted into equation (10) to obtain three-dimensional coordinate.

$$\begin{bmatrix} X_i \\ Y_i \\ 1 \end{bmatrix} = inv(H_{z1})(\lambda_i x_i' - v_z Z_1) \quad (10)$$

Algorithm 4: Outline reconstruction algorithm

Condition: Given the four control points and two control points towards the vertical direction in each image, the gray images of reconstruction object contours, the Z-axis value corresponding to reference height.

Objectives: Restore the three-dimensional coordinates of the object, and the flow chart is shown in Figure 6. Steps:

- a) Initialize variables: $Z = 0$, and set iterative incremental dz ;
- b) According to the Z-axis value corresponding to the reference height, adopt the height algorithm below to calculate the height value of the object;
- c) If $Z \leq Z_H$, repeat to run step d; otherwise skip to step e;
- d) Restore the three-dimensional coordinates of the Z-level sections. First, calculate the Z-level space control points, and then calculate the Z-level overlay intersection of the slice. Finally, restore the Z-level the three-dimensional coordinates of the slice. $Z=Z+dz$, and skip to step b.
- e) Output the three-dimensional contour model of the reconstructed object.

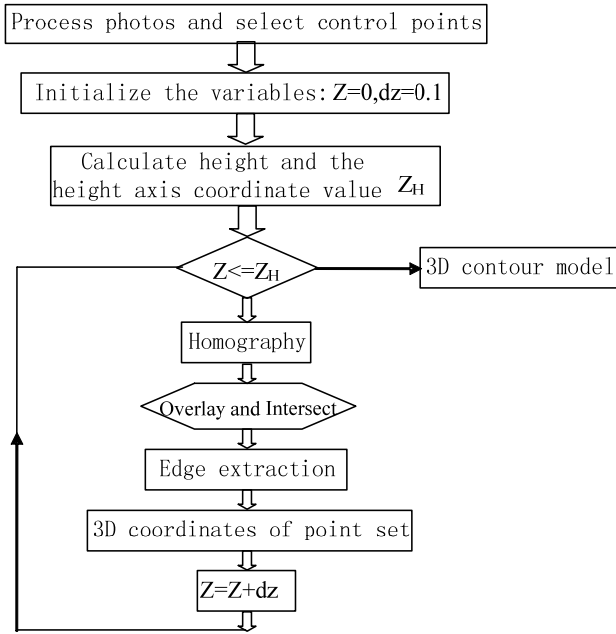


Figure 6. The flow chart of three dimensional reconstruction from 2D slicing plane.

Algorithm 5: The algorithm of the reconstructed object height

Condition: Given the four control points and two control points towards the vertical direction in each image, the gray images of reconstruction object contours.

Objective: Calculate the actual height of the object, as well as Z-axis coordinate value corresponding to the height, and the flow shown is in Figure 7. Steps:

- a) Determination of the reference height;
Create a coordinate system, and determining the Z-axis coordinate value corresponding to a reference height from the control points.
- b) Set the variables: $varZ=0$, incremental Zd , the range of the upper limit $ZMax$, and the lower limit $ZMin$;
- c) Repeat steps c to carry out a wide range of approximation to the highest point of the object;
When $Z=varZ$, algorithm 2 are adopted to overlay and intersect to obtain the slice. Judge the slice area if it is greater than zero. When greater than zero, $varZ = varZ + Zd$, repeat step c. Equal to 0, then set $ZMax=varZ$, $ZMin=varZ-Zd$, and skip to step d.
- d) Set the variables $varZ=(ZMin+ZMax)/2$, the upper limit of $High=ZMax$, the lower limit of $Low=ZMin$, and $threshold$;
- e) obtained the range $[ZMin, ZMax]$ in step c, repeat step e, approaching the highest point of the object in small range;

If $High-Low < threshold$, Skip to step f, otherwise algorithm 2 are adopted to overlay and intersect to obtain the slice.

The first case is that greater than zero, then $Low=varZ$. The second case is that equal to 0, then set $High=varZ$. $varZ=(Low+High)/2$, repeat step e.

f) According to the Z-axis coordinate value corresponding to the reference height, calculate the height

corresponding to $varZ$, namely the reconstructed height of the object, and output actual height and $varZ$.

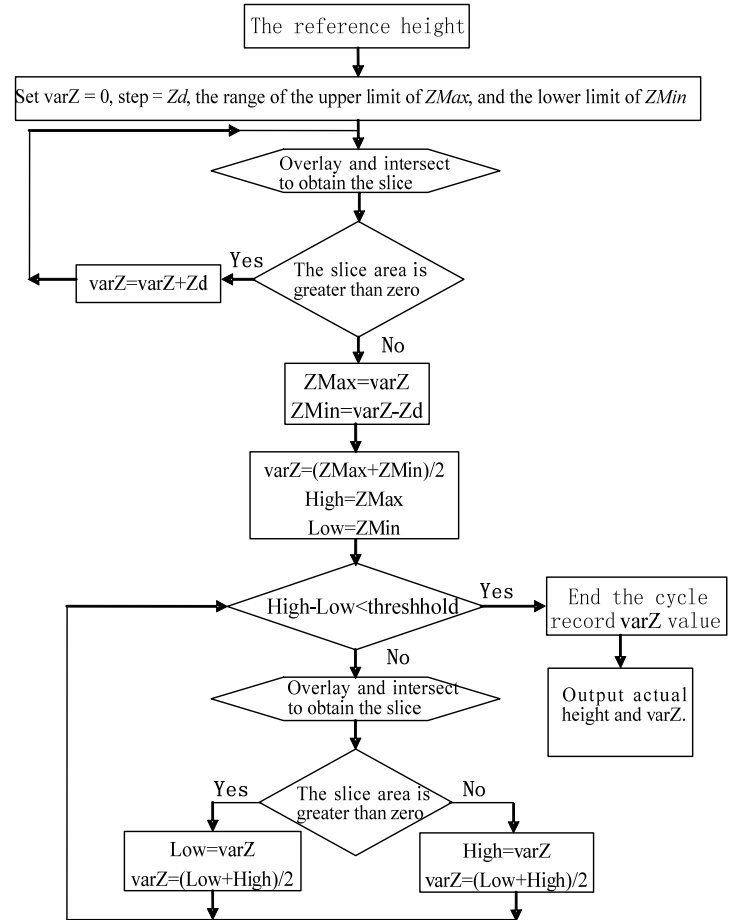


Figure 7. The flow chart of the calculation of the reconstructed object height

IV. EXPERIMENT

The experiment takes a boundary marker and a sculpture for example to verify the proposed algorithm in the paper. Take a set of images of reconstructed object in different angles. The control points, reference height selection and the coordinates for each object are seen in Figure 8. The intersection results of several images for the first layer and the middle layer is seen in Figure 9, The intersection shape extraction compared to the reference image is showed in Figure 10. The marked points distribution of sculpture is showed in Figure 11 , and the accuracy comparison of the reconstructed objects is showed in table 1 and table 2 respectively.



a) a boundary marker



b) a sculpture

Figure 8. Control points, reference height selection and the coordinates construction for each object

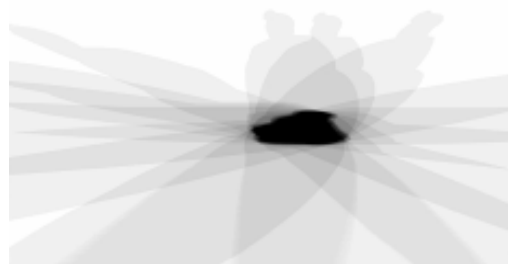
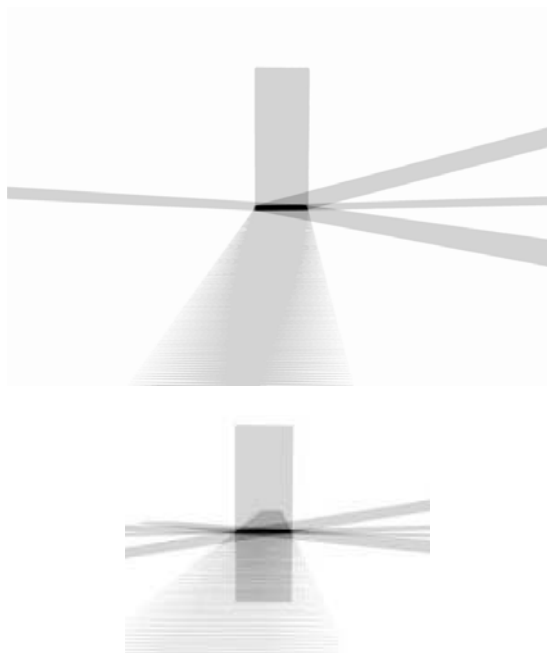
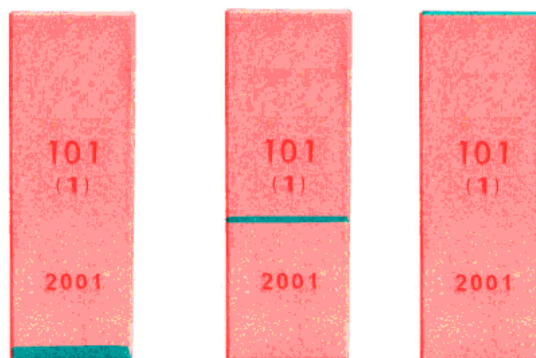


Figure 9. The intersection results of several images for the first layer and the middle layer



a) a boundary marker



b) Sculpture

Figure 10. The intersection shape extraction compared to the reference image



Figure 11. The distribution of marked points.

TABLE I.
ACCURACY OF EACH EDGE FOR THE BOUNDARY MARKER

Edge side	Length 1 /cm	Length 2/cm	Length 3/cm	Length 4/cm	Height/cm
Reconstructed object					
Calculated length	35.2	20.3	36.4	20.2	101.2
Actual length	36.0	20.0	36.0	20.0	100.0
Absolute error	-0.8	0.3	0.4	0.2	1.2

TABLE II.
ACCURACY OF EACH MARKED POINT FOR SCULPTURE

Point to point	Calculating distance/cm	Actual distance/cm	Absolute error/cm	Relative error
1 to 2	48.1	48.7	0.6	0.012
1 to 3	58.1	59.1	1.0	0.017
1 to 4	50	51.3	1.3	0.025
1 to 6	31	29.3	-1.7	0.058
2 to 4	64.5	63.4	-1.1	0.017
3 to 4	32	32.8	0.8	0.024
3 to 5	59.3	60.5	1.2	0.020
4 to 5	32	33.1	1.1	0.033
4 to 6	55.4	57	1.6	0.028

In the reconstruction process, all the images captured should at least include the outline of the entire reconstructed object. The more Images imply more abundant reconstruction information, while the more time-consuming and labor-intensive to deal. Generally speaking, it needs fewer images for the regular object with the obvious outline to complete the reconstruction, while it needs more images for irregular object in order to obtain more detailed characteristics of the more overlap. From table 1 and table 2, we can see that the accuracy is good.

V. CONCLUSION

The advantage of the reconstruction method proposed by this paper is obvious. Firstly, this method requires no

camera calibration or the estimation of the fundamental matrix; hence, it reduces the computational complexity by eliminating the requirement for abundant conjugate points. Secondly, the aspect of interest is selected by its silhouette. Thirdly, the paper proposes the height algorithm of a reconstructed object by the scene reference height. It only needs a small amount of images when it just needs height without reconstructing the shape of the object. In the case of some of the less precision, this approach is more flexible. This makes the non-measurement camera in the entire three-dimensional data acquisition, and it is very convenient, fast and greatly reduces production costs and workload. The premise of the reconstruction adding vanishing point is to ensure that a straight-line imaging is still a straight

line. Otherwise it is unable to complete the reconstruction, such as fish-eye lens. For the panoramic images, it needs to modify the projection way to apply this method proposed by the paper, and which is our next research work.

ACKNOWLEDGMENT

This research is supported by the project of Yunnan provincial education department (NO.2012C198), National Natural Science Foundation (No. 41301442, 41201418), and Pecuniary aid of Yunnan Province basic research for application (2013fz127)

REFERENCES

[1] R. Hartley and A. Zisserman. Multiple View Geometry in computer Vision - second edition. Cambridge Un. Press, 2004.

[2] S. Khan, P. Yan, and M. Shah. A homographic framework for the fusion of multi-view silhouettes. IEEE Int. Conf. on Computer Vision, pages: 1-8, 2007.

[3] Thomas Luhmann. Close range photogrammetry for industrial applications, ISPRS Journal of Photogrammetry and Remote Sensing 65 (2010): 558-569

[4] Wada, T., Wu, X., Tokai, S. and Matsuyama, T., 2000. Homography based parallel volume intersection: Toward real-time volume reconstruction using active cameras. In: IEEE International Workshop on Computer Architectures for Machine Perception.

[5] K. Wong and R. Cipolla. Structure and motion from silhouettes. IEEE,ICCV, 2001.

[6] S. Lazebnik, Y. Furukawa, J. Ponce. Projective Visual Hulls. IJCV 2006.

[7] Khan, S. and Shah, M., 2006. A multiview approach to tracking people in crowded scenes using a planar homography constraint. In: European Conf. on Computer Vision.

[8] Kelly, P., Beardsley, P., Cooke, E., O'Connor, N. and Smeaton, A., 2005. Detecting shadows and low-lying objects in indoor and outdoor scenes using homographies. In: IEE International Conference on Visual Information Engineering.

[9] Zhang, Z. and Hanson, A., 1996. 3d reconstruction based on homography mapping, in Proc. ARPA96

[10] Zhang, Q., Wang, H. and Wei, S., 2003. A new algorithm for 3d projective reconstruction based on infinite homography. In: Machine Learning and Cybernetics.

[11] Yun, Y., Kim, S., Lee, S., Kim, D. and Choi, J., 2006. Threedimensional reconstruction of an object using three-planar homography of a single image. In: Optical Engineering, Vol. 45.

[12] Khan, S., Yan, P. and Shah, M., 2007. A homographic framework for the fusion of multi-view silhouettes. In: IEEE Int. Conf. on ComputerVision.

[13] Po-Lun Lai and Alper Yilmaz, 2008. PROJECTIVE RECONSTRUCTION OF BUILDING SHAPE FROM SILHOUETTE IMAGES ACQUIRED FROM UNCALIBRATED CAMERAS. In:ISPRS Conf, Beijing.



Shuai Liu received the B.S. , M.S. and PhD degrees in Geographic Information System from Central South University , Changsha, China, in 2003, 2006 and 2011 respectively. From March 2007 to May 2011, he was a research associate at National Geomatics Center of China. Currently, he is working at School of Engineering of Honghe University, Mengzi, China. His research interest

covers computer vision, 3D modeling and virtual augmented reality.



Lingli Zhao received the B.S. degree in Computer Science in 2001 from Central South University, and received M.S. and PhD degrees in Geographic Information System from Central South University, Changsha, China, in 2003, 2006 and 2011 respectively. Currently, she is working at School of Engineering of Honghe University, Mengzi, China. Her

research interest covers 3D modeling, data integration and data mining.



Junsheng Li received the B.S. degree in Physical in 1982 from Yunnan University, and received M.S. degree in information and electronic from Yunnan University, Kunming, China in 1997. Currently, he is working at School of Engineering of Honghe University, Mengzi, China. His research interest covers computer network.



Li Ma received the B.S. and PhD degrees in Photogrammetry and Remote Sensing from Wuhan University, Hubei, China in 2003 and 2011 respectively. From July 2004 to June 2011, he was a research associate at National Geomatics Center of China. Currently, he is working at Changjiang Institute of Survey, Planning, Design and Research,

Wuhan, China. His research interests cover photogrammetry engineering and remote sensing applications.